PROCEEDINGS OF SCIENCE

EndoTOFPET-US: an endoscopic Positron Emission Tomography detector for a novel multimodal medical imaging tool

Daniele Cortinovis[*†]
DESY and University of Hamburg
E-mail: daniele.cortinovis@desy.de

The EndoTOFPET-US collaboration aims to integrate Time-Of-Flight PET with ultrasound endoscopy in a novel multimodal device, capable to support the development of new biomarkers for prostate and pancreatic tumors.
The detector consists of two parts: a PET head mounted on an ultrasound probe and an external PET plate, placed outside the body in coincidence with the PET head. The gamma ray detection is performed by scintillating crystals with Silicon PhotoMultiplier (SiPM) readout. Analog SiPM are used in the external plate, while new dedicated multi-digital SiPM have been developed for the internal probe, which also involves other technological solutions due to the high level of miniaturization.
The spatial resolution of 1 mm for the PET image requires small crystal size, and therefore high channel density. Moreover, the detector is designed to achieve an unprecedented Coincidence Time Resolution (CTR) of 200 ps FWHM, essential for effective background rejection. Compared to conventional PET scanner, the unusual asymmetric design requires a tracking system with a resolution better than 1 mm, and poses new issues for detector simulation. In addition, the image reconstruction has to cope with the limited field of view. The detector design and the characterization of single components are presented.

53rd International Winter Meeting on Nuclear Physics
26-30 January 2015
Bormio, Italy

[*]Speaker.
[†]On behalf of the EndoTOFPET-US collaboration.

PoS(Bormio2015)045

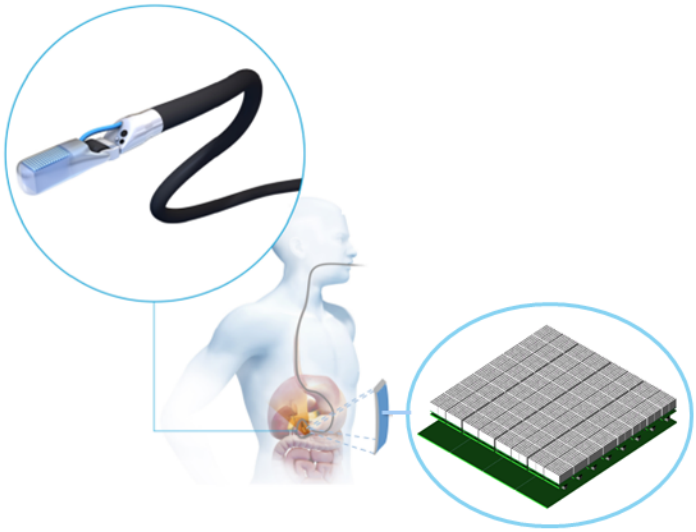

Figure 1: The EndoTOFPET-US detector with a magnification of the pancreatic endoscope (top circle) and the external plate (bottom circle).

1. Introduction

Pancreatic carcinoma is among the most aggressive cancer, it is practically asymptomatic during its first stage of development and very resistant to current therapies. The diagnosis is usually carried out with computer tomography (CT) and ultrasound (US), but often it comes too late: the 5-year survival rate is lower than 2% [1]. On the other hand, despite prostate cancer is the most common cancer among males, it can be treated with high probability of success if detected at early stages. In this case imaging procedures usually include magnetic resonance tomography and US. The EndoTOFPET-US project [2] aims to advance the imaging techniques for these diseases, therefore improving the diagnosis capability and the treatment efficacy. This goal is pursued with the development of a novel multimodal imaging tool, which combines TOFPET and US in a unique system able to test the performance of newly developed specific biomarkers for pancreatic and prostate tumors. The EndoTOFPET system, depicted in Figure 1, consists of a PET head extension mounted on a commercial ultrasound probe placed in coincidence with a PET plate positioned outside the patient body. The endoscopic approach together with the small pixel dimension allow to achieve a spatial resolution of 1 mm for the metabolic PET image. Moreover, the quality of the image can be enhanced by the TOF technique. The demanding coincidence time resolution of 200 ps FHMW allows to reject coincidences occurred outside the region of interest, therefore reducing the noise in the reconstructed image. The EndoTOFPET-US will push forward the limits of the current PET scanners, provided that new challenges are overcome. The detector asymmetry requires the development of dedicated simulation software while the limited field of view demands advanced image reconstruction algorithm. The extreme miniaturization poses challenges for electronics and mechanic integration. Finally, a tracking system must provide the position of the two PET detectors with a precision better than 1 mm.

2. The external PET plate

The external PET plate (Figure 2 and 3) is a square of 23 x 23 cm^2 made of 256 detector modules (Figure 4c). Each module consists of an array of 4x4 LYSO:Ce crystals (Figure 4a), with individual volume of 3.5 x 3.5 x 15 mm^3 wrapped in a 3M Vikuiti reflector foil. The crystal matrices are coupled to an analog 4x4 SiPM array (Hamamatsu MPPC S12643-050CN(X), Figure 4b), which exploits the Through Silicon Via (TSV) technology, leading to less dead space and a reduced connection length as compared to conventional wire-bonded SiPM. Each SiPM in the array has an active area of 3 x 3 mm^2 with 3464 pixels, while the distance between two consecutive SiPMs in the array is 0.6 mm.

The SiPM readout is provided by custom made ASICs, which have been developed within the collaboration. Two options are currently available: the TOFPET [3] and the STiC [4]. In both versions the timing information is obtained with the leading edge technique, with a time jitter less than 20 ps. The energy information is given by the time-over-threshold (ToT) method. Given the detector design, the ASICs have to face high channel density ($\sim$4000 channels in 20x20 cm^2), low power consumption (<20 mW/channel) and provide SiPM bias tuning capability of at least 0.5 V.

STiC is a mixed mode 64-channel ASIC chip in UMC 0.18 μm CMOS technology, designed for time of flight measurements in both HEP and medical imaging applications. It provides either single-ended or differential SiPM readout. The timestamps from the input signal are processed by an embedded TDC with a time resolution better than 20 ps. The digitized data are then transferred via a 160 MBit LVDS serial link with 8/10-bit-encoding.

The TOFPET-ASIC is a 64-channels chip in 25 mm^2 designed in a standard CMOS 0.13 μm technology. One edge of the chip is free of pins, allowing to combine two chips in a single 128 channels module. The connection to the SIPM is single-ended and the timing and ToT information obtained by a dual thresholds system are processed by an analogue TDC with 50 ps binning. The digitized data is packed in frames and sent to the DAQ system via LVDS links, with a maximum bandwidth of 640 MBit/s.

The first external plate prototype has been equipped with STiC v3.0 chips, which are mounted on the analog front end boards (a-FEBs) and then placed on the cooling plates.

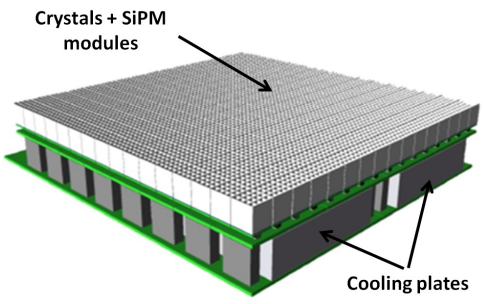

Figure 2: The design of the EndoTOFPET-US external plate

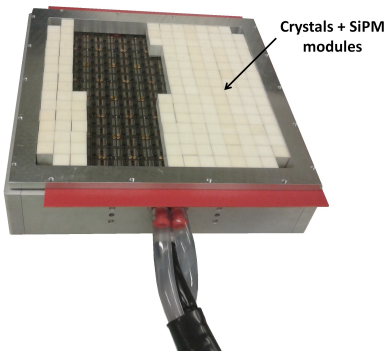

Figure 3: Assembly of the external plate, partially filled with the detctor modules.

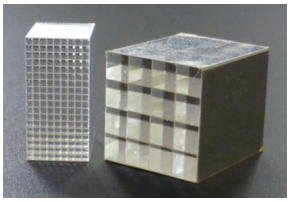

(a) LYSO:Ce crystal matrix for the internal probe (left) and for the external plate (right).

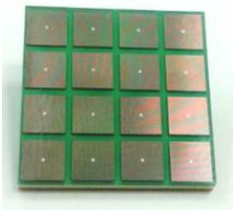

(b) The 4x4 SiPM array for the external plate.

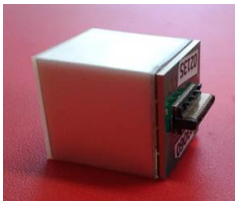

(c) The detector module for the external plate (crystal matrix glued to the SiPM array).

Figure 4: EndoTOFPET-US detector components

3. The internal probe

Figure 5 shows the internal probe for the prostate case: a miniaturized PET detector attached at the end of a trans-rectal US endoscopic probe (Hitachi medical systems EUP-U533). The PET extension has the same cross section as the US probe (23 mm diameter) and the scintillating crystals, photodetector, electronics and cooling are integrated in such a small volume. The crystals have an individual volume of 0.71 x 0.71 x 15 mm^3 and they are grouped in two matrices of 9 x 16 crystals each. Each crystal is wrapped with reflector foil and individually coupled to a custom made multi-channel digital SiPM (md-SiPM) [5]. The md-SiPM is divided in clusters, each of which is made of 416 single photon avalanche diodes (SPAD) of 30 x 50 μm^2 each. In contrast to the operation of a standard analog SiPM, the outputs from the SPADs are not summed up together but read out by individual counters, one per SPAD. In principle it could be also possible to incorporate a TDC per SPAD, allowing to register the time of arrival of each detected photon and therefore reach the Cramér-Rao [6] [7] lower bound for timing uncertainty. However, the fill factor would decrease because of the space required by the additional electronics, reducing the effective light output and in turn worsen the CTR [8]. A good trade off between sufficient fill factor and high time resolution is achieved with 48 TDCs per cluster. The pancreatic PET probe will be very similar to the prostate case, but the dimension will be even smaller (15 mm diameter).

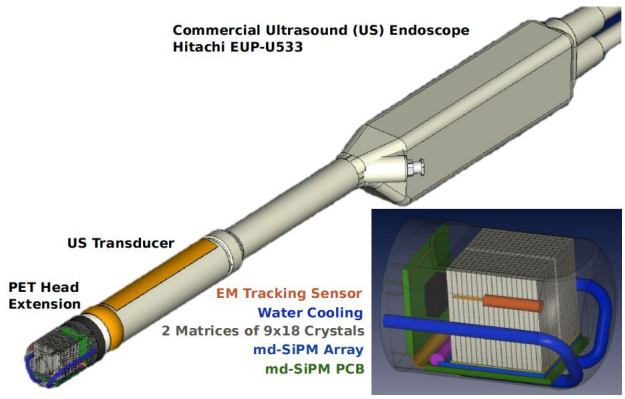

Figure 5: The internal probe (for prostate) of the EndoTOFPET-US detector.

4. Components characterization

4.1 Characterization of SiPM arrays and crystal matrices

All the 256 SiPM arrays for the external plate have been characterized before the assembly with the corresponding crystal matrices. Each SiPM is measured in terms of gain, breakdown voltage, Dark Count Rate (DCR) and correlated noise, which includes after-pulse and optical crosstalk. The SiPM performances depend on the excess bias voltage applied, therefore the determination of the breakdown voltage of each SiPM is of critical importance. Moreover, the ASIC tuning range for the SiPM bias voltage is limited at 0.5 V, therefore the breakdown voltage spread in each SiPM array must be limited to this value. All the 256 SiPM arrays received meet this requirement. One of the SIPM drawbacks is DCR. This has a negative impact on the coincidence time resolution, because the chip threshold for the time information is set at the noise level. Therefore a DCR limit of 3 MHz at 25 ^{o}C has been agreed with the SiPM vendor, and after extensive quality assurance tests, only 2% of received SiPM arrays have been rejected due to excessive DCR. Average DCR for the 4096 detector channels is (1.4 $\pm$ 0.4) MHz at 25 ^{o}C. It is known that also temperature influences SiPM behavior, therefore the temperature dependence of breakdown voltage and DCR has been obtained for a sample SiPM.
As well as the SiPM arrays, also all the 256 crystal matrices have been characterized in regards of light yield and energy resolution. As shown in other studies [9], high light yield improves the coincidence time resolution. With the help of the MiniACCOS setup [10], an average light yield of about 32000 Ph/MeV is obtained when the crystal arrays are coupled to the PMT with optical grease. After the crystal matrices are glued to the SiPM arrays, the light output and energy resolution for the 511 keV photon is measured, as well as the CTR for all the detector modules (crystal + SiPM). The 511 keV light output shows a good uniformity among the 4096 detector channels (about 7% dispersion), while the average energy resolution is about 13% (Figure 6), in agreement with the minimum requirement of 20%. The CTR of all the detector modules is measured with respect to a common reference module. The NINO [11] is used as readout chip, and the chip thresholds, temperature and SiPM excess bias are kept fixed for all the channels in order to compare the results. As shown in Figure 7, an average CTR of 239.5 ps FWHM is obtained.

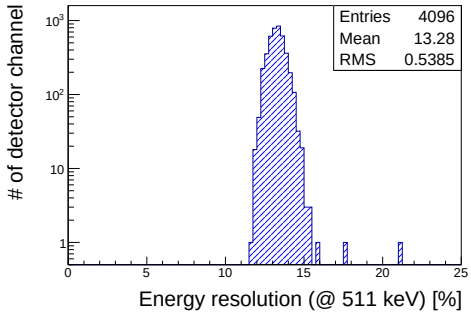

Figure 6: Energy resolution at 511 keV for all the channels.

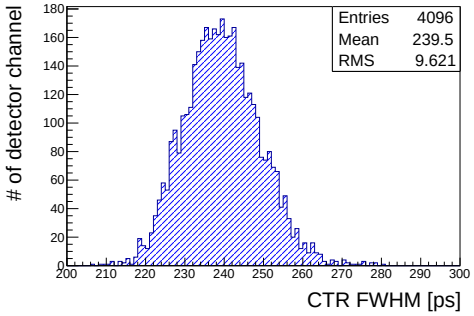

Figure 7: The CTR distribution of all channels pairs, at 19 ^{o}C and at 2.5 V excess bias.

4.2 ASICs characterization

Both STiC and TOFPET ASICs have been developed and characterized. The ASICs performance complies with the specifications and the integration in the first EndoTOFPET-US prototype has started. As shown in Figure 8, CTR of 215 ps FWHM has been obtained with STiC v3.0 used as readout of two single crystals (3x3x15 mm^3) coupled to 3x3 mm^2 Hamamatsu MPPCs. On the other hand, the single pixel time resolution has been evaluated for TOFPET, resulting in 211 ps FWHM.

4.3 Multi-digital SiPM characterization

First prototypes of the md-SiPM have been produced and tested. Figure 9 summarizes the results obtained on the firsts md-SiPM prototypes. A PDE of 12.5 % is obtained when the SPADs are operated at 3 V excess bias. Similarly to the analog SiPM, the DCR increases with the temperature and therefore deteriorates the time resolution. An advantage of the md-SiPM is the possibility to mask noisy pixels, therefore significantly reducing the DCR with a minimum impact on the PDE (as shown in the plot, half DCR is obtained with 10% masking). The timing jitter of a single SPAD and for a cluster (416 SPADs) is measured as well. Results show a SPTR of 121 ps for a single SPAD and 179 ps for the entire sensor (laser and clock jitter subtracted).

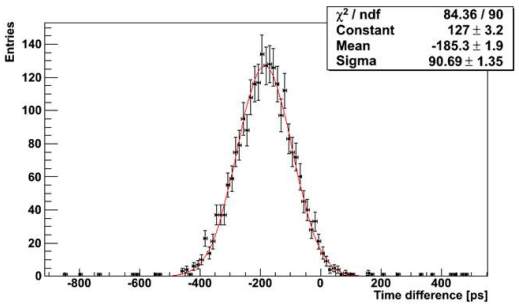

Figure 8: A CTR of about 215 ps FWHM has been obtained with STiC as readout of single crystals (3x3x15 mm^3) coupled to 3x3 mm^2 Hamamatsu MPPC

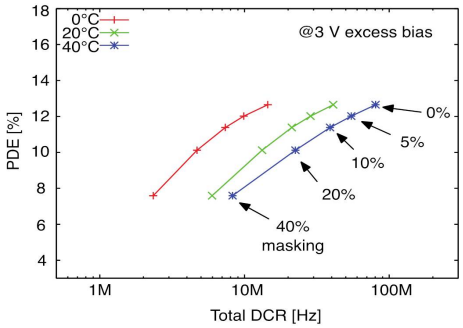

Figure 9: Characterization of the md-SiPM. The PDE and the DCR is evaluated at 3 V excess bias at different temperatures and masking configurations.

5. Data acquisition

In the external plate, a field programmable gate array (FPGA) is installed on each digital front end board (d-FEB). Each FPGA collects the digital inputs from the ASICs and transmits it to the DAQ via 1.6 Gb/s links. The readout system for the external plate is designed for a maximum event rate of 40 MHz (160 kHz per channel). In the internal probe, the events from the md-SiPM are collected by a FPGA mounted inside the probe, with a maximum data rate of 625 kpcs. The DAQ system [12] is installed on a PCIe card, which merges the data from the external plate and internal probe and performs a coarse coincidence selection with a time window of 12.5 ns. Besides the coincidence selection, the DAQ output also includes the detector position information from the

tracking system. Moreover, the DAQ is responsible for the correct configuration and the monitoring of the different devices of the system. A schematic of the DAQ infrastructure is shown in Figure 10.

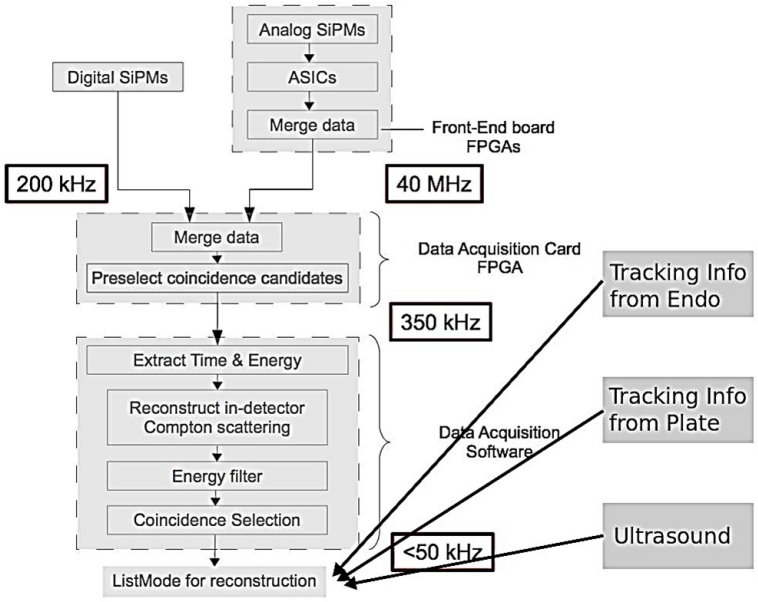

Figure 10: Flowchart of the event processing chain handled by the DAQ.

6. Detector simulation and image reconstruction

The custom developed image reconstruction software is based on the maximum-likelihood expectation-maximization (ML-EM) algorithm. It includes the TOF information in a histogram based algorithm and accounts for the free-hand nature of the acquisition. Moreover, due to the application in image guided surgery, the image reconstruction is performed on powerful Graphical Processing Units (GPUs), providing the PET image in order of minutes.
The expected performance of the EndoTOFPET-US detector is studied with simulations based on the GAMOS toolkit (Geant4-based Architecture for Medicine-Oriented Simulations). Studies on simple phantoms suggest that the spatial resolution of 1 mm is within reach and a scan time of 10 minutes is sufficient. Some rotation of the detector significantly improves the overall quality of the PET image [13]. Figure 11 shows the image reconstruction of a prostate lesion from full body PET/CT DICOM data. This data have been provided by the Nuclear Medicine department of Klinikum Rechts der Isar (Munich), and it has been obtained with 140 MBq injected into the patient.

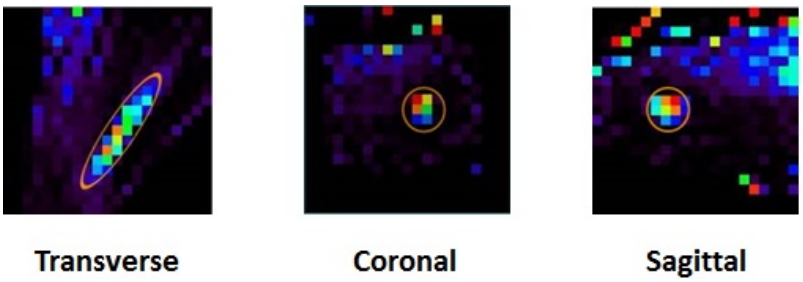

Figure 11: Reconstructed image of the prostate lesion (inside the circles) using the full body PET/CT DICOM data after 3 minutes acquisition. Actual dimensions of the three images is 4.2 x 4.2 cm^2, with voxels of 2 mm.

7. Conclusions and outlook

The EndoTOFPET-US project aims to build a novel multimodal medical imaging tool, able to test newly developed specific biomarkers for prostate and pancreatic cancer. All the detector components have been produced and characterized, showing performances up to the requested specifications. A first detector prototype is now under construction and commissioning.

Acknowledgements

The author thanks the EndoTOFPET-US collaboration for the privilege of representing it at this conference. This research project has received funding from the European Union 7th Framework Program (FP7/ 2007-2013) under Grant Agreement No. 256984 (EndoTOFPETUS) and is supported by a Marie Curie Early Initial Training Network Program (PITN-GA-2011-289355-PicoSEC-MCNet).

References

[1] R. Ported, J. Kaplan (Eds.), *The Merck Manual for Healthcare Professionals, 18th edition, retrieved March 8th, 2013*,

[2] EndoTOFPET-US Proposal: *Novel multimodal endoscopic probes for simultaneous PET/ultrasound imaging for image-guided interventions*, European Union 7th Framework Program (FP7/2007-2013) under Grant Agreement No. 256984, Health-2010.1.2-1.

[3] M.D Rolo et al., *TOFPET ASIC for PET applications*, JINST (2013) 8 C02050.

[4] Wei Shen et al., *STiC - A mixed Mode Chip for SiPM ToF Applications*, IEEE NSS/MIC Conf. Record (2012) N14-37.

[5] S. Mandai and E. Charbon, *Multi-channel digital SiPMs: Concept, analysis and implementation*, Nuclear Science Symposium and Medical Imaging Conference (NSS/MIC), 2012 IEEE, pages 1840-1844, 2012.

[6] Harald Cramér, *Mathematical Methods of Statistics*, ISBN: 9780691005478, Princeton University Press, 23.03.1999.

[7] C. R. Rao, *Information and accuracy attainable in the estimation of statistical parameters*, Bull. Cal. Math. Soc., Vol. 37 (1945), 81-91.

[8] S. Seifert, HT. van Dam and D.R. Schaart, *The lower bound on the timing resolution of scintillation detectors*, Phys. Med. Biol. 57 (2012) 1797.

[9] Y. Shao, *A new timing model for calculating the intrinsic timing resolution of a scintillator detector*, Phys. Med. Biol. 52 (2007) 1103-1117.

[10] J. Trummer et al., *Scintillation Properties of LuYAP and LYSO Crystals Measured with MiniACCOS, an Automatic Crystal Quality Control System*, IEEE NSS/MIC Conf. Record (2005) 2807-2810.

[11] F. Anghinolfi et al., *NINO: An ultra-fast and low-power front-end amplifier/discriminator ASIC designed for the multigap resistive plate chamber*, Nucl. Instrum. Meth. A 533 (2004) 183.

[12] R. Bugalho et al., *EndoTOFPET-US data acquisition system*, Journal of Instrumentation, 8(02):C02049, 2013.

[13] M. Zvolsky et al., *Monte-Carlo Simulation and Image Reconstruction for an Endoscopic TOFPET Detector*, IEEE Nuclear Science Symposium and Medical Imaging Conference, Seattle, USA, November 2014